

# Stellar indices and kinematics in Seyfert 1 nuclei

Luis Jiménez-Benito,<sup>1★</sup> Angeles I. Díaz,<sup>1</sup> Roberto Terlevich<sup>2†</sup> and Elena Terlevich<sup>3‡</sup>

<sup>1</sup>*Departamento de Física Teórica C-XI, Universidad Autónoma de Madrid, Cantoblanco, 28049 Madrid, Spain*

<sup>2</sup>*Institute of Astronomy, Madingley Road, Cambridge CB3 0HA*

<sup>3</sup>*Instituto Nacional de Astronomía, Óptica y Electrónica, Tonantzintla, Puebla, Mexico*

Accepted 2000 May 13. Received 2000 May 13; in original form 1999 July 5

## ABSTRACT

We present spectra of six type 1 and two type 2 Seyfert galaxies, a starburst galaxy and a compact narrow-line radio galaxy, taken in two spectral ranges centred around the near-infrared Ca II triplet ( $\sim 8600 \text{ \AA}$ ), and the Mgb stellar feature at  $5180 \text{ \AA}$ . We measured the equivalent widths (EWs) of these features and the Fe<sub>52</sub> and Fe<sub>53</sub> spectral indices.

We found that the strength of the infrared Ca II triplet (CaT) in type 1 Seyfert galaxies with prominent central point sources is larger than what would be expected from the observed strength of the blue indices. This could be explained by the presence of red supergiants in the nuclei of Seyfert 1 galaxies. On the other hand, the blue indices of these galaxies could also be diluted by the strong Fe II multiplets that can be seen in their spectra.

We have also measured the stellar- and gas-velocity dispersions of the galaxies in the sample. The stellar velocity dispersions were measured using both the Mgb and CaT stellar features. The velocity dispersion of the gas in the narrow-line region (NLR) was measured using the strong emission lines [O III]  $\lambda\lambda 5007, 4959$  and [S III]  $\lambda 9069$ . We compare the gas- and star-velocity dispersions and find that the magnitudes of both are correlated in Seyfert galaxies.

Most of the Seyfert 1 galaxies that we observe have stellar-velocity dispersions somewhat greater than that of the gas in the NLR.

**Key words:** galaxies: active – galaxies: kinematics and dynamics – galaxies: nuclei – galaxies: Seyfert – galaxies: stellar content.

## 1 INTRODUCTION

The presence of young massive stars in the nuclear regions of Seyfert galaxies was strongly suggested by the detection of the near-infrared absorption Ca II triplet ( $\sim 8600 \text{ \AA}$ ; CaT) in a sample of active galactic nuclei (AGN) by Terlevich, Díaz & Terlevich (1990, hereafter TDT90). This stellar feature depends strongly on gravity and only weakly on metallicity, and is known to be specially strong in young red supergiants (Jones, Alloin & Jones 1984; Díaz, Terlevich & Terlevich 1989). The analysis of this feature led TDT90 to conclude that strong starbursts should be present in the nuclei of type 2 Seyferts because, despite the weakness or dilution observed in the blue stellar absorption lines, the CaT was found to be very strong in the nuclear spectra of the 12 galaxies of this type that were observed. Moreover, the only three Seyfert 1 galaxies included in their sample also show CaT in absorption, suggesting at least some contribution by a young stellar population.

Subsequent infrared spectroscopy ( $1.5\text{--}2.3 \mu\text{m}$ ) of normal and active galaxies performed by Oliva et al. (1995) allowed them to conclude that the Seyfert 2 nuclei of their sample were compatible with evolution from a precursor starburst. They also found that the  $1.6\text{--}2.3 \mu\text{m}$  stellar continuum of Seyfert nuclei is too red to be accounted for by a non-thermal continuum, but is compatible with reprocessed radiation from hot dust.

Cid Fernandes & Terlevich (1992, 1993, 1995), in a critical analysis of the simple unified scenario (Antonucci 1993), proposed that the observed strong CaT in Seyfert type 2 galaxies, with a strong blue optical continuum with the absence of broad lines and combined with the low continuum polarization, were the result of the presence in the nuclear region of unpolarized starlight from very young stars, i.e. a nuclear/circumnuclear starburst or star-forming toroid. This simple suggestion seems to enable us to overcome most of the difficulties faced by the basic unified model for Seyfert 2 galaxies, while preserving its attractive features.

Schmitt, Storchi-Bergmann & Cid Fernandes (1999) have recently found that the spectra of many Seyfert 2s can be modelled by the sum of the spectra of a young ( $\sim 100 \text{ Myr}$ ) and an old ( $\sim 10 \text{ Gyr}$ ) stellar cluster, and that these models reproduce the observations better than the traditional ones consisting of a blue

★ E-mail: luis@delta.ft.uam.es

† Visiting professor at INAOE, Puebla, Mexico.

‡ Visiting fellow at the Institute of Astronomy, Cambridge.

featureless continuum (BFC) and an old stellar population, thus confirming the suggestions of Cid Fernandes & Terlevich.

The question concerning the origin of the nuclear continuum in Seyfert 2s has given rise to the search for young stars in their nuclei. Heckman et al. (1997) and González Delgado et al. (1998) have presented high-resolution ultraviolet images, taken with the *Hubble Space Telescope* (*HST*), of four Seyfert 2 galaxies, finding compact nuclear starbursts in all of them. They have also found spectral features from young hot stars in the ultraviolet spectra of these four galaxies. Their main conclusion is that, in all the galaxies they have studied, the observed continuum is exclusively a result of a nuclear/circumnuclear young starburst and that the energy emitted by the nuclear starburst is, at least, of the same order as the energy produced by the buried active galactic nucleus. Powerful starbursts have also been found in the nuclei of several LINERS by Colina et al. (1997) and Maoz et al. (1998), and very recently in a quasi-stellar object (QSO) by Brotherton et al. (1999).

If the results presented above can be generalized to all type 2 Seyferts, then, we could conclude that nuclear starbursts ought to play an important role in the total energy emitted in their nuclear regions. Furthermore, as Seyfert 1 and 2 galaxies are not physically different kinds of object in unified models, but are the consequence of a different viewing angle, one can conclude that if nuclear starbursts are found to be energetically important in Seyfert 2s, they should also be important in Seyfert 1s.

However, the starbursts in Seyfert 1 nuclei, if present, may be somewhat different from those in Seyfert 2: the narrow H $\alpha$  and [N II] emission in Seyfert 2 galaxies is more extended than in Seyfert 1 hosts (Pogge 1989; González Delgado & Pérez 1993). Also, the galaxies with type 2 Seyfert nuclei have enhanced infrared emission from their discs compared with the emission from type 1 nuclei, or with the emission from normal spiral galaxies (Maiolino et al. 1995). From their near-infrared observations, Oliva et al. (1995) found that the  $M/L$  ratio in Seyfert 1s is similar to the ratio shown by normal early-type spiral galaxies, whereas this ratio is found to be lower in Seyfert 2s, pointing to younger stellar populations. Also, González Delgado et al. (1997) found that circumnuclear star-forming rings are more common in Seyfert 2s than in Seyfert 1s. Moreover, the few ultraviolet *HST* images that exist of type 1 Seyferts show point sources rather than compact starbursts in their nuclei.

In this paper, we use the fact that the nuclear light output in Seyfert 1 galaxies has little contamination from the surrounding bulge to search for signatures of a nuclear starburst. If, for example, strong CaT absorptions were detected in the unresolved nuclear component, because of the limited surface brightness, they could not be a result of bulge contamination. It should be possible to detect a starburst signature even in the presence of a dominant nuclear component. In other words, if the result from Heckman et al. (1997) and González Delgado et al. (1998) can be generalized – i. e. that the luminosity of the starburst is equal to or larger than that of the AGN – then the surface brightness of the stellar population giving rise to the CaT feature should be much higher than that from the old bulge component, in order for it to be detected on top of the dominant AGN spectrum, and therefore should be detectable in the presence of the nuclear continuum.

We have looked for signatures of young stars in the optical/near-infrared spectra of six type 1 Seyfert galaxies. Although, in principle, the ultraviolet would be the best spectral band to detect absorptions from young stars, the strong broad line region (BLR) contamination at the wavelengths of the stronger stellar features

**Table 1.** Observational parameters.

$\lambda_c$	5100 Å	8700 Å
Dates	1991 May 3–4	1991 May 3–4
Telescope	WHT	WHT
Spectrograph	ISIS	ISIS
Grating	600B	316R
Detector	CCD TEK 1	CCD TEK 2
Filter	–	CG495
Spectral range	4706–5607 Å	7983–9573 Å
Dispersion	0.73 Å pixel <sup>−1</sup>	1.39 Å pixel <sup>−1</sup>
Spatial scale	0.3 arcsec pixel <sup>−1</sup>	0.3 arcsec pixel <sup>−1</sup>
Slit width	1.04 arcsec	1.04 arcsec

([C IV]  $\lambda$ 1550 Å and [Si IV]  $\lambda$ 1400 Å) makes this method not viable. On the other hand, as discussed by TDT90, the region around the near-infrared CaT is relatively free of strong emissions.<sup>1</sup>

It is known that the stellar kinematics in the nuclei of Seyfert galaxies are similar to that of normal spiral galaxies, because both types of galaxy follow the same Faber–Jackson relation (TDT90; Nelson & Whittle 1996). It is also known that the gas motions in the narrow line region (NLR) of Seyfert galaxies seem to be dominated by the gravitational field of the bulge, as the width of the [O III]  $\lambda$  5007 emission line is correlated with the nuclear stellar velocity dispersion (Wilson & Heckman 1985; TDT90; Nelson & Whittle 1996). TDT90 found a small population of type 2 Seyfert galaxies with gas velocities much larger than the stellar velocities. The existence of this population was confirmed by Nelson & Whittle (1996).

The kinematics of the stars and gas in the nuclei of our sample galaxies was also studied in this paper, improving previous results by adding six new Seyfert 1 galaxies to the samples referred to above.

## 2 OBSERVATIONS AND DATA REDUCTION

High-resolution long-slit spectra from the galaxies of our sample were obtained in 1991 May during two observing nights with the William Herschel Telescope (WHT) at the Roque de los Muchachos Observatory, on the Spanish island of La Palma. Details concerning the set-up for the observations can be found in Table 1. We used the two arms of the ISIS spectrograph to take, simultaneously, two spectra of each galaxy in different spectral ranges. We observed 11 galaxies. One of the galaxies (the radio galaxy Hydra A) is not included in this work because of the poor quality of the spectra obtained for it. Two different exposures of 30 min (three in some objects, see Table 2) were taken for each galaxy. This allowed us to clean the spectra of cosmic ray events. Besides the galaxies of the sample, we also observed several stars for flux calibration, for the subtraction of water vapour bands and for velocity measurements.

The reduction of the data was performed using standard tools in the IRAF package. The reduction process was performed fully in two dimensions and consisted of several steps: bias subtraction, flat-fielding, cosmic-rays cleaning, wavelength and flux calibration and, finally, sky subtraction. This last step was the most

<sup>1</sup> The O I  $\lambda$ 8400 Å and the [Fe II]  $\lambda$ 8617 Å lines are exceptions to this. The first line is broad and prominent in luminous Seyfert 1 galaxies, whereas the second one is narrow and seems to be present in some starburst and Seyfert 2 galaxies.

**Table 2.** Observations and galaxy sample.

Galaxy	Alternate Designation	RA (1950)	Dec. (1950)	PA (°)	Night	$\lambda_c$ (Å)	Exposure (s)
NGC 4235	IC 3098	12 <sup>h</sup> 14 <sup>m</sup> 36 <sup>s</sup>	+07° 28' 09"	70	2	5100	3600
						8700	3600
NGC 5940	UGC 9876	15 <sup>h</sup> 28 <sup>m</sup> 51 <sup>s</sup>	+07° 37' 38"	70	2	5100	3600
						8700	3600
NGC 6104	UGC 10309	16 <sup>h</sup> 14 <sup>m</sup> 40 <sup>s</sup>	+35° 49' 50"	83	1	5100	3600
						8700	3600
Mk 270	NGC 5283	13 <sup>h</sup> 39 <sup>m</sup> 41 <sup>s</sup>	+67° 55' 28"	70	2	5100	3600
						8700	3600
Mk 423	MCG 6-25-72	11 <sup>h</sup> 24 <sup>m</sup> 07 <sup>s</sup>	+35° 31' 34"	170	1	5100	5400
						8700	5400
Mk 759	NGC 4152	12 <sup>h</sup> 08 <sup>m</sup> 05 <sup>s</sup>	+16° 18' 41"	35	2	5100	3600
						8700	3600
Mk 766	NGC 4253	12 <sup>h</sup> 15 <sup>m</sup> 55 <sup>s</sup>	+30° 05' 27"	108	1	5100	5400
						8700	5400
Mk 885	–	16 <sup>h</sup> 29 <sup>m</sup> 43 <sup>s</sup>	+67° 29' 06"	90	1	5100	3600
						8700	3600
Mk 1098	–	15 <sup>h</sup> 27 <sup>m</sup> 37 <sup>s</sup>	+30° 39' 24"	70	2	5100	3600
						8700	3600
3C305	IC 1065	14 <sup>h</sup> 48 <sup>m</sup> 18 <sup>s</sup>	+63° 28' 36"	57	1,2	5100	3600
						8700	3600

difficult one, at least for the near-infrared spectra, because, in the spectral range covered by these spectra, there are many atmospheric absorption and emission bands. The emission features were eliminated by subtracting spectra of the sky from the spectra of the galaxies. The elimination of the OH and water absorption bands was achieved by dividing by the spectrum of a standard star. This procedure is not perfect and has two main problems. The first problem is that the atmospheric conditions change during the night. The second problem is that the absorption lines of the star cannot be eliminated when they coincide with the atmospheric absorption lines. For this reason, when dividing the galaxy spectra by the stellar spectrum, weak pseudo-emission lines often appear, which have their origin in the photospheric absorption lines in the stellar spectrum. In Fig. 1 we can see two examples of the results of the correction procedure. In Mk 1098, observed during the first night, we can see that the original strong absorption bands appear, after division, like weak ‘emission bands’. This can be caused by changes in the atmospheric conditions during the night. In Mk 423, observed during the second night, weak narrow ‘emission lines’ can be seen caused by absorption lines in the spectrum of the star.

One-dimensional spectra were extracted at the end of the reduction process by summing the 10 central pixels and this corresponds to 3 arcsec. The average seeing was about 1 arcsec.

The spectra were not corrected for galactic reddening.

### 3 NOTES ON INDIVIDUAL OBJECTS

The main physical properties of the 10 galaxies in the sample are given in Table 3. The redshift of the sample covers a range 0.007–0.041 and therefore a factor of 4 in size. The nuclear blue spectra of the sample can be seen in Figs 2 and 3. In this last figure, the spectra are enlarged in order to show the stellar features in the nuclei of the galaxies. The near-infrared spectra are shown in Fig. 4. The CaT is seen in absorption in all of the nuclei, even in that of Mk 766, where it is detected also in emission.

#### 3.1 NGC 4235

NGC 4235 is classified as a Seyfert 1 galaxy in the literature

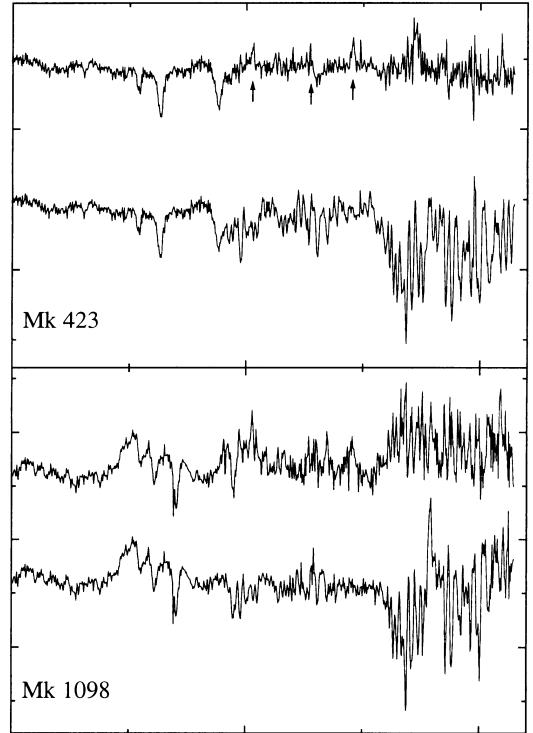


**Figure 1.** Elimination of atmospheric absorption bands. In both frames the upper spectrum is the one corrected for atmospheric absorption. In Mk 1098 (bottom panel) the correction method caused broad ‘emission bands’ to appear. On the contrary, in Mk 423 (upper panel) only weak and narrow ‘emission lines’ (marked with arrows) appear after the correction procedure.

(Abell, Eastmond & Jenner 1978; Morris & Ward 1988). It is a nearly edge-on spiral galaxy and its nuclear emission is strongly reddened by the dust in the spiral arms of the galaxy (Abell et al. 1978). It has a spatially resolved nucleus, bisected by a dust lane (Malkan, Gorjian & Tam 1998), and extended radio emission spread on both sides of the galaxy (Colbert et al. 1996a) with a compact radio core (Ulvestad & Wilson 1984b; Kukula et al.

**Table 3.** Physical properties of the sample. Column (2) gives the nuclear type of the galaxy taken from the literature. Column (3) tells us whether the nucleus is spatially resolved or not in *HST* images from Malkan et al. (1998). The data of columns (4)–(7) are from de Vaucouleurs et al. (1991) (RC3). The values in column (8) have been calculated with data in columns (6) and (7). We have derived the values in column (9) from the empirical formulae of Simien & de Vaucouleurs (1986) and the data in column (8).

Galaxy (1)	Type (2)	Resolved (3)	Morphology (4)	$T$ (5)	$cz$ (6)	$B_r^o$ (7)	$M_{B_r^o}$ (8)	$M_{\text{bulge}}$ (9)
NGC 4235	Sy 1	yes	SA(s)a	$1.0 \pm 0.3$	$2343 \pm 33$	11.93	$-20.5$	$-19.5 \pm 0.6$
NGC 5940	Sy 1	no	SBab	$2.0 \pm 0.9$	$10\,172 \pm 21$	14.13	$-21.5$	$-20.3 \pm 2.8$
NGC 6104	Sy 1.5	yes	S?	–	$8382 \pm 50$	14.04	$-21.2$	–
Mk 270	Sy 2	yes	S0?	$-2.0 \pm 1.7$	$3165 \pm 86$	14.12	$-19.0$	$-18.5 \pm 1.5$
Mk 423	Sy 1.9	yes	S0?	–	$9652 \pm 11$	14.63	$-20.9$	–
Mk 759	HII	yes	SAB(rs)c	$5.0 \pm 0.3$	$2066 \pm 46$	12.38	$-19.8$	$-17.3 \pm 1.8$
Mk 766	Sy 1.5	no	SB(s)a	$1.0 \pm 0.6$	$3819 \pm 25$	13.74	$-19.8$	$-18.8 \pm 1.3$
Mk 885	Sy 1.5	yes	S?	–	$7593 \pm 30$	14.86	$-20.2$	–
Mk 1098	Sy 1.5	–	S?	–	$10\,710 \pm 49$	–	–	–
3C305	NLRG	–	SB0	$-2.0 \pm 0.8$	$12\,423 \pm 53$	14.43	$-21.7$	$-21.1 \pm 0.7$

1995). The galaxy presents optical emission lines extended along the major axis (Pogge 1989; Colbert et al. 1996b).

### 3.2 NGC 5940

NGC 5940 is a barred spiral galaxy with an unresolved point source in the nucleus (Malkan et al. 1998). It is a prototypical Seyfert 1 galaxy with broad permitted emission lines, like H $\beta$  and O I  $\lambda$ 8446, and it is also a strong Fe II emitter. The multiplets of Fe II form two big bumps in the spectrum of NGC 5940, one around 4600 Å in the blue edge of the spectrum (see Fig. 3), and the other one between 5150 Å and 5250 Å. The first of these bumps is caused by multiplets (37) and (38), whereas the second one is caused by multiplets (42), (48) and (49) (Osterbrock 1977). Besides strong emission lines, many stellar absorption features can be seen in its spectra: the Mg b, Fe<sub>52</sub> and Fe<sub>53</sub> features are clearly visible. The near-infrared spectrum of NGC 5940 is affected by problems with sky subtraction, and the third line of the CaT has nearly been lost. A comparison with older spectra (Morris & Ward 1988) indicates that the galaxy has not suffered violent changes in the last years.

### 3.3 NGC 6104

NGC 6104 shows a spatially resolved nucleus, a nuclear bar and a strongly disturbed spiral pattern that can appear like a ring in low-resolution images (Malkan et al. 1998). There are no good quality images of the external region: the image in the Digital Sky Survey presents a highly disturbed appearance.

Our spectrum shows that it could be classified as a Seyfert 1.5–1.8 galaxy. Most striking in this spectrum is the shape of the spectral lines. The broad component of H $\beta$  shows an asymmetrical double-peaked shape, and the forbidden emission lines are very narrow and are only marginally resolved.

### 3.4 Mk 270

This is a nearly face-on S0/E galaxy. It shows filaments, wisps and dust lanes in its inner regions (Malkan et al. 1998). It has extended [O III] and H $\alpha$  emission elongated at PA = 58° (Haniff, Wilson & Ward 1988; Mulchaey, Wilson & Tsvetanov 1996). It also has two weak radio components on both sides of the nucleus elongated in the same direction as the extended optical emission (Ulvestad & Wilson 1984a; Kukula et al. 1995).

### 3.5 Mk 423

Mk 423 is classified in the literature as a type 1.9 Seyfert galaxy (Osterbrock 1981). Our spectra confirm that H $\beta$  has no broad component.

This galaxy is interacting with a nearby companion (Malkan et al. 1998). In the literature it is often included among Markarian galaxies with multiple nuclei (e.g. Nordgren et al. 1995). Mk 423 and its companion both have extended emission line regions seen in [O III] and H $\alpha$  (Rudy, Cohen & Puetter 1985). Our blue spectrum of the companion suggests an H II galaxy classification. The radio core of Mk 423 is partially resolved (Ulvestad 1986).

One interesting feature in the spectrum of this galaxy is the broad absorption wings of H $\beta$  that suggest the presence of young main-sequence stars. Rudy et al. (1985) found a moderately strong ultraviolet continuum in the 1200–2000 Å spectrum but no signs of broad emission lines. This ultraviolet continuum emission could be produced by the same young stars that produce the broad absorption wings of H $\beta$ .

### 3.6 Mk 759

Mk 759 is the only starburst galaxy in our sample, and is included for comparison purposes. H $\beta$  has broad absorption wings, which indicate the presence of young stars.

### 3.7 Mk 766

Mk 766 is a barred spiral galaxy. *HST* images (Malkan et al. 1998) show filaments, wisps and irregular dust lanes around an unresolved nucleus. It has a partially resolved radio core with an extension to the north. The total size of the source is  $\sim 200 \text{ pc } h^{-1}$  (Ulvestad & Wilson 1984a). The polarization angle of the light emitted by Mk 766 is approximately perpendicular to the radio axis (Goodrich 1989). The optical emission is extended (González Delgado & Pérez 1996; Mulchaey et al. 1996) through a region the total size of which is greater than that of the radio source. In X-rays, it is variable on a few hours time-scale, and presents a strong soft X-ray excess (Molendi, Maccacaro & Schaeidt 1993). Molendi & Maccacaro (1994) asserted that the soft X-rays excess and the hard X-ray emission are produced by two distinct mechanisms. Nandra et al. (1997) reported the detection of an Fe K $\alpha$  line in the X-ray spectrum.

It is classified as a narrow line Seyfert 1 galaxy (Osterbrock &

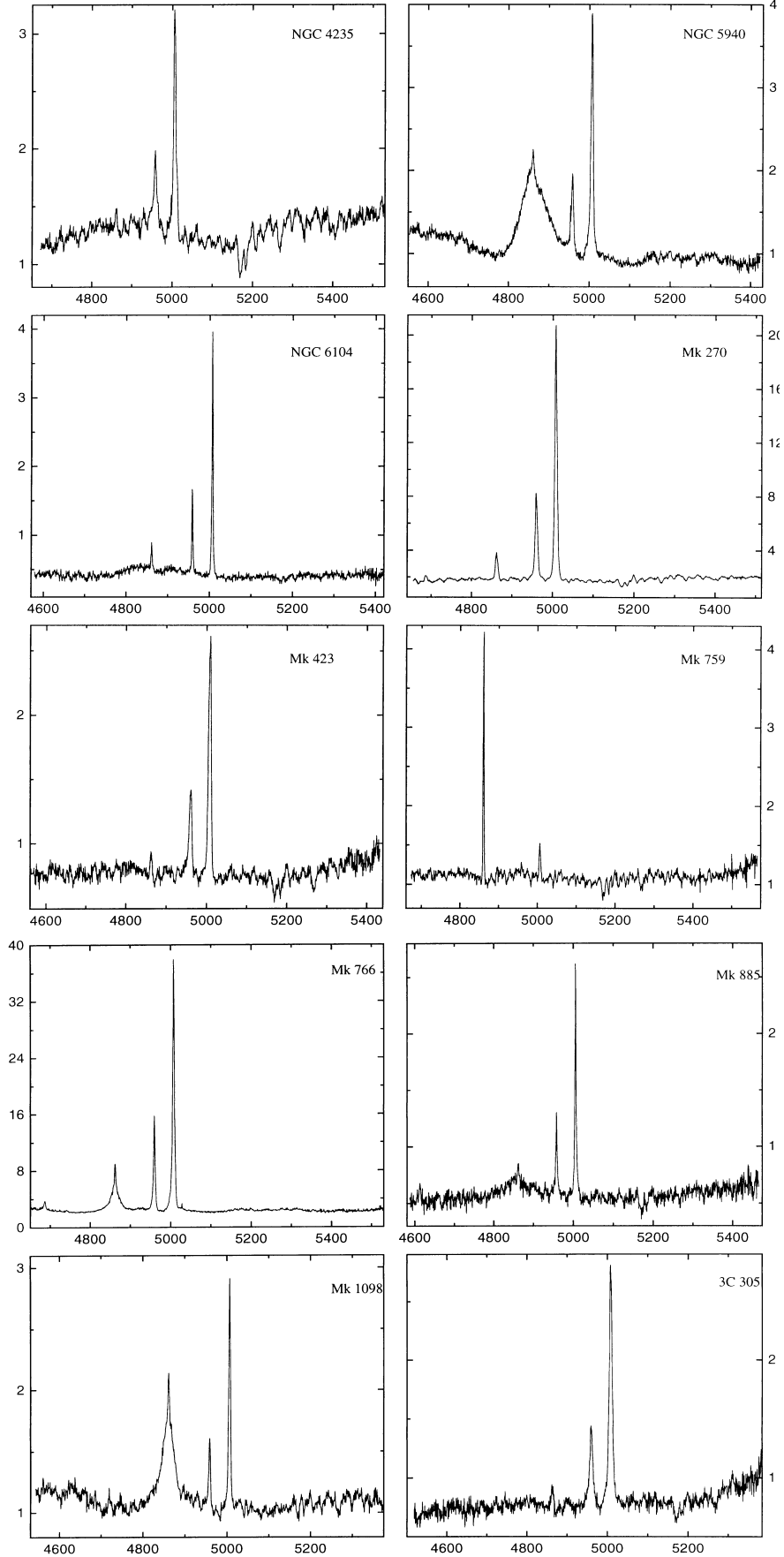


**Figure 2.** Blue spectra of the galaxies of the sample. The flux is in units of  $10^{-15} \text{ erg cm}^{-2} \text{ s}^{-1}$  and the wavelengths are in Å. Note that the scale in each spectrum is different.

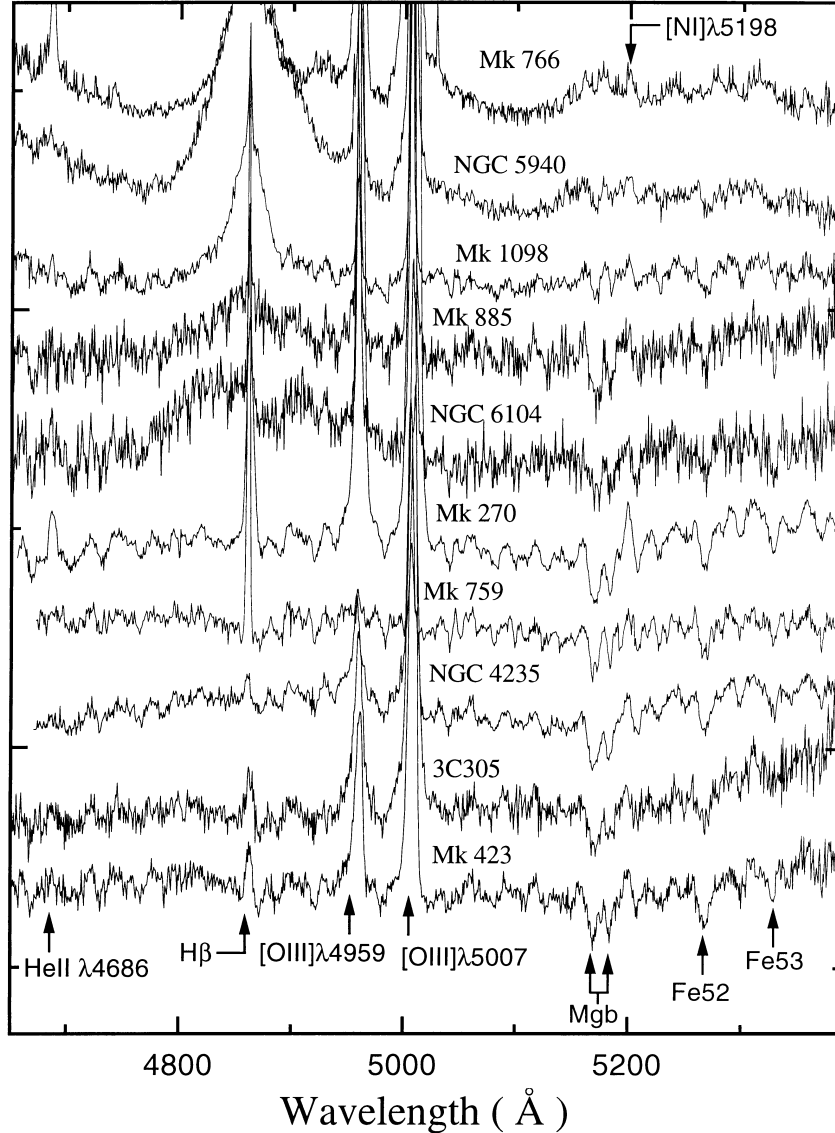


**Figure 3.** Enlarged blue spectra showing the stellar absorption features of the galaxies in the sample.

Pogge 1985). Much work has been performed on its emission spectrum (e.g. Veilleux 1991), with the most thorough work performed by González Delgado & Pérez (1996). Mk 766 is the only galaxy in the sample that shows CaT in emission (Persson 1988). Interestingly, in our spectrum, and also in the one by González Delgado & Pérez (1996), the CaT is also seen in absorption (see Fig. 4).

### 3.8 Mk 885

Mk 885 is a barred spiral galaxy (Xanthopoulos & De Robertis 1991), and is classified as a 1.5 Seyfert galaxy. Our spectra of this galaxy are not very good, but we can confirm the results of Osterbrock & Dahari (1983) that the nuclear spectrum has stellar absorption features. Its nucleus is spatially resolved (Malkan et al. 1998) at *HST* resolution.

### 3.9 Mk 1098

There are no good images of this galaxy available and its morphological parameters are not well known. The nuclear

spectrum of Mk 1098 looks like that of NGC 5940, but with weaker and narrower permitted emission lines than the lines of the latter. It is a moderately strong Fe II emitter. The most striking feature in the spectra of this galaxy is the strange shape of the feature that forms the O I  $\lambda 8446$  emission line and the CaT. Although part of this could be a result of poor sky subtraction (see Fig. 1), the CaT might also be in emission in the nucleus.

### 3.10 3C 305

This galaxy is the only radio galaxy in our sample. Its blue spectrum is very similar to the the spectrum of Mk 423. The results will be presented elsewhere.

## 4 MEASUREMENTS

### 4.1 Line strengths

#### 4.1.1 Definitions

Our central interest is to measure the strength of optical and

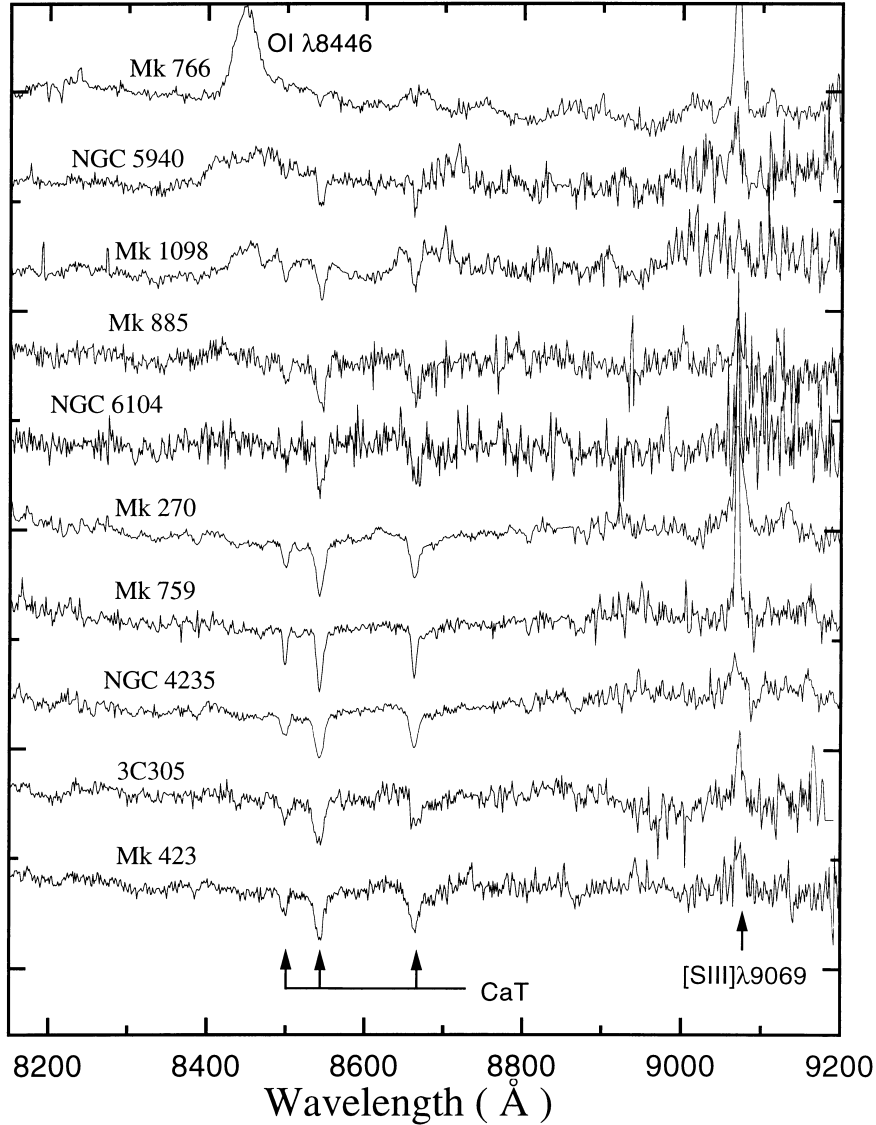


**Figure 4.** Enlarged near-infrared spectra showing the CaT. This feature is seen in absorption in all galaxies and even in Mk 766 where CaT is also seen in emission.

near-infrared stellar absorption features. To do this, we follow the approach of TDT90 and measure ‘pseudo-equivalent widths’.

The definition of the pseudo-equivalent width of a spectral index is

$$W_c \equiv \Delta\lambda_c \left( 1 - \frac{F_c^L}{F_c^C} \right),$$

where  $\Delta\lambda_c$  is the width of the central window and  $F_c^L$  is the mean flux in that bandpass.  $F_c^C$  is the value of the pseudo-continuum in the central wavelength  $\lambda_c$ . The pseudo-continuum is defined by interpolation of the flux in two continuum bandpasses:

$$F_c^C \equiv \frac{F_b^C - F_a^C}{\lambda_b - \lambda_a} \lambda_c + \frac{F_a^C \lambda_b - F_b^C \lambda_a}{\lambda_b - \lambda_a},$$

where  $F_b^C$  and  $F_a^C$  are the mean values of the flux in the continuum windows and  $\lambda_a$  and  $\lambda_b$  are their central wavelengths. Hereafter, pseudo-equivalent widths will be called equivalent widths (EWs) for simplicity.

Table 4 gives the definitions of the relevant continuum and central bandpasses. The definitions corresponding to the blue indices are taken from the Lick system (e.g. Gorgas et al. 1993), whereas the definitions of the CaT are taken from TDT90.

The errors of the EWs were calculated using a simplified version of the photon statistic method. The measured rms values of the spectra in the continuum bandpasses were taken as the errors of the mean values of the continuum in these bands. The errors of the EWs were then calculated by propagating errors from the above expressions (Palacios et al. 1997). These errors are thus only lower limits.

#### 4.1.2 Broadening correction

The velocity dispersion of the stars broaden the absorption lines in the spectra of galaxies; therefore, the central bandpasses of the indices may not contain the complete feature. A correlation exists between the velocity dispersion of a given galaxy and the EWs of

the absorption lines in the integrated spectrum and a correction for this effect is needed. For more details see TDT90.

#### 4.1.3 Emission line effects

The  $Mg_2$  index is more affected by the presence of emission lines in AGN than the Mgb, so we have measured Mgb.

The [N I]  $\lambda 5198$  doublet inside the red continuum bandpass of the Mgb index still remains a problem. One method to solve it is to eliminate the line of [N I] (Goudfrooij & Emsellem 1996); another method is to use optional bandpasses. The correction factors for the optional definitions of the Mgb index are very close to unity.

To measure the EW of the Mgb, two optional bandpasses, defined in Palacios et al. (1997), were used. Without applying any correction, the two measurements were averaged to find the EW of the Mgb index. To test the validity of the method, the emission lines in the spectra of two of the galaxies, NGC 4235 and Mk 270, were eliminated. Of all of the galaxies in the sample, these are the ones that have the oldest stellar population. Their spectrum looks like that of a red giant star. Three spectra of K-type stars, taken the same night as the spectra of the galaxies, were combined to form a template calibration star. Using an iterative procedure (Cardiel, Gorgas & Aragón-Salamanca 1998) the ranges affected by emission lines in the spectrum of the galaxies were fitted and replaced. The measurements obtained with this method in Mk 270 and NGC 4235 are the same as the results obtained by using our optional windows.

In the near-infrared spectra, the problems are caused by the presence of the broad emission line O I  $\lambda 8446$  in the blue continuum bandpass of the CaT indices, and by residuals of the sky subtraction in the red bandpasses.

Fortunately, the broad emission O I  $\lambda 8446$  was a problem only in two galaxies: NGC 5940 and Mk 1098. For these galaxies, we fitted two Gaussians to the broad component of  $H\beta$  in both galaxies, and eliminated the O I line by taking these Gaussians as an initial fit. The O I emission line in NGC 5940 could be properly subtracted with only small modifications to the original Gaussians. Mk 1098 O I line could only be fitted by one of the Gaussians.

The red bandpasses of the CaT indices were manually cleaned in all of the spectra to eliminate the residuals of the sky subtraction.

Mk 766 is a special case. It shows many broad emission lines in the near-infrared (O I  $\lambda 8446$  and some lines of the Paschen series; even the CaT is in emission). The stellar features in the blue are

also completely diluted. No stellar feature could therefore be measured in this galaxy.

#### 4.1.4 Results

The EWs of the different lines for the galaxies in the sample are given in Table 5, both corrected and non-corrected for broadening. This correction is smaller than the error in all galaxies. In the analysis of the next section, the corrected values are used. For Mgb we use the results obtained with optional bandpasses. For consistency with previous work (TDT90), hereafter we call the CaT index the sum of the EWs of the second and third lines of the CaT: CaT (2 + 3). The EW of the third line of the CaT in NGC 5940 is only a lower limit because of the effect of the atmospheric absorption bands on this line (see Fig. 4).

## 4.2 Velocity dispersions

### 4.2.1 Stellar velocity dispersions

To measure stellar velocity dispersions, we used the cross-correlation method described by Tonry & Davis (1979). This method gives small systematic errors when directly applied, as can be seen in Fig. 5. In this figure we plot the velocity dispersion, computed for a broadened stellar spectrum applying the cross-correlation method, versus the width of the Gaussian used to broaden it. It is clear from the figure that, no matter how the correlation function is filtered, the method always gives small errors. To correct this effect, sixth-order empirical correction curves were calculated (Nelson & Whittle 1995; Palacios et al. 1997).

Several correlation functions were calculated for every galaxy. We filtered each function in different ways, measured the width of the respective central peaks and applied the corresponding correction curve to each measurement. Finally, the velocity dispersion of the galaxy was obtained by averaging all of the measurements.

Two independent measurements of the velocity dispersion of each galaxy were obtained using the blue and the near-infrared spectra, respectively.

### 4.2.2 Gas velocity dispersions

The width of the emission lines  $H\beta$ , [O III]  $\lambda\lambda 5007, 4959$  and

**Table 4.** Definitions of the atomic indices. The definition of the Mgb index is the one of the Lick system. The optional Mgb indices, 1 and 2, have optional red windows defined by Palacios et al. 1997. The indices CaT 1, 2 and 3 measure the EW of each of the three lines of the CaT, as defined by TDT90.

Index	Continuum blue bandpass (Å)	Central bandpass (Å)	Continuum red bandpass (Å)
Fe <sub>52</sub>	5235.50–5249.25	5248.00–5286.75	5288.00–5319.25
Fe <sub>53</sub>	5307.25–5317.25	5314.75–5350.50	5356.00–5364.75
Mgb	5144.50–5162.00	5162.00–5193.25	5193.25–5207.00
Mgb opt. 1	5144.50–5162.00	5162.00–5193.25	5207.00–5221.00
Mgb opt. 2	5144.50–5162.00	5162.00–5193.25	5220.00–5234.00
CaT 1	8447.50–8462.50	8483.00–8513.00	8842.50–8857.50
CaT 2	8447.50–8462.50	8527.00–8557.00	8842.50–8857.50
CaT 3	8447.50–8462.50	8647.00–8677.00	8842.50–8857.50



**Table 5.** EWs of the features in the galaxies of the sample.

Index	NGC 4235 EW (Å)	NGC 5940 EW (Å)	NGC 6104 EW (Å)	Mk 270 EW (Å)	Mk 423 EW (Å)	Mk 759 EW (Å)	Mk 885 EW (Å)	Mk 1098 EW (Å)	3C 305 EW (Å)
$H\beta_{\text{broad}}$	> -35	~ -85	~ -40	—	—	—	~ -35	~ -45	—
[O III] $\lambda 5007$	$-13.6 \pm 0.9$	$-26 \pm 1$	$-35 \pm 2$	$-81 \pm 4$	$-23 \pm 1$	$-2.0 \pm 0.1$	$-17 \pm 1$	$-10.6 \pm 0.6$	$-27.7 \pm 0.6$
Fe <sub>52</sub>	$2.7 \pm 0.3$	$0.7 \pm 0.3$	$1.6 \pm 0.6$	$2.5 \pm 0.3$	$2.4 \pm 0.4$	$1.8 \pm 0.3$	$1.5 \pm 0.5$	$1.8 \pm 0.3$	$2.2 \pm 0.4$
Fe <sub>53</sub>	$2.4 \pm 0.3$	$0.8 \pm 0.4$	$1.2 \pm 0.8$	$3.1 \pm 0.3$	$2.3 \pm 0.5$	$1.2 \pm 0.4$	$1.9 \pm 0.8$	$1.1 \pm 0.3$	$1.8 \pm 0.7$
Mgb	$4.6 \pm 0.3$	$0.9 \pm 0.3$	$2.7 \pm 0.6$	$5.3 \pm 0.5$	$4.1 \pm 0.4$	$2.6 \pm 0.4$	$3.8 \pm 0.5$	$0.7 \pm 0.3$	$3.5 \pm 0.3$
Mgb opt. 1	$4.1 \pm 0.3$	$0.5 \pm 0.3$	$2.9 \pm 0.6$	$4.2 \pm 0.4$	$3.3 \pm 0.4$	$2.1 \pm 0.3$	$3.0 \pm 0.5$	$0.3 \pm 0.3$	$3.1 \pm 0.3$
Mgb opt. 2	$4.2 \pm 0.2$	$0.3 \pm 0.3$	$3.0 \pm 0.5$	$4.2 \pm 0.3$	$3.2 \pm 0.3$	$2.2 \pm 0.3$	$3.2 \pm 0.5$	$0.2 \pm 0.3$	$3.1 \pm 0.3$
CaT (1)	$1.3 \pm 0.1$	$1.3 \pm 0.2$	$1.3 \pm 0.3$	$1.3 \pm 0.1$	$0.9 \pm 0.2$	$1.2 \pm 0.1$	$1.5 \pm 0.4$	$2.3 \pm 0.2$	$1.5 \pm 0.2$
CaT (2)	$3.3 \pm 0.1$	$1.7 \pm 0.2$	$2.9 \pm 0.3$	$3.7 \pm 0.1$	$3.3 \pm 0.2$	$3.3 \pm 0.1$	$3.7 \pm 0.4$	$2.0 \pm 0.2$	$3.6 \pm 0.2$
CaT (3)	$2.9 \pm 0.2$	$1.3 \pm 0.2$	$2.6 \pm 0.3$	$2.9 \pm 0.1$	$3.3 \pm 0.3$	$2.7 \pm 0.1$	$3.3 \pm 0.4$	$2.2 \pm 0.2$	$2.2 \pm 0.2$
CaT (2 + 3)	$6.3 \pm 0.3$	$3.0 \pm 0.4$	$5.5 \pm 0.6$	$6.6 \pm 0.2$	$6.6 \pm 0.5$	$6.0 \pm 0.2$	$7.0 \pm 0.7$	$4.2 \pm 0.3$	$5.8 \pm 0.4$
Fe <sub>52</sub> ( $\sigma = 0$ )	$2.9 \pm 0.4$	$0.8 \pm 0.3$	$1.7 \pm 0.8$	$2.7 \pm 0.4$	$2.6 \pm 0.5$	$1.8 \pm 0.3$	$1.6 \pm 0.6$	$1.8 \pm 0.3$	$2.5 \pm 0.8$
Fe <sub>53</sub> ( $\sigma = 0$ )	$2.6 \pm 0.3$	$0.8 \pm 0.4$	$1.3 \pm 0.9$	$3.3 \pm 0.4$	$2.5 \pm 0.5$	$1.2 \pm 0.5$	$2.0 \pm 0.8$	$1.1 \pm 0.3$	$2.0 \pm 0.8$
Mgb ( $\sigma = 0$ )	$5.0 \pm 0.4$	$1.0 \pm 0.4$	$3.0 \pm 0.6$	$5.8 \pm 0.5$	$4.5 \pm 0.5$	$2.7 \pm 0.4$	$4.1 \pm 0.5$	$0.7 \pm 0.4$	$4.0 \pm 0.5$
Mgb opt. 1 ( $\sigma = 0$ )	$4.4 \pm 0.4$	$0.5 \pm 0.3$	$3.1 \pm 0.6$	$4.4 \pm 0.4$	$3.6 \pm 0.4$	$2.1 \pm 0.3$	$3.2 \pm 0.6$	$0.3 \pm 0.3$	$3.4 \pm 0.4$
Mgb opt. 2 ( $\sigma = 0$ )	$4.5 \pm 0.3$	$0.4 \pm 0.3$	$3.2 \pm 0.6$	$4.4 \pm 0.4$	$3.4 \pm 0.4$	$2.2 \pm 0.3$	$3.4 \pm 0.5$	$0.2 \pm 0.3$	$3.4 \pm 0.4$
CaT (1) ( $\sigma = 0$ )	$1.3 \pm 0.2$	$1.3 \pm 0.2$	$1.3 \pm 0.4$	$1.3 \pm 0.1$	$0.9 \pm 0.2$	$1.2 \pm 0.1$	$1.5 \pm 0.4$	$2.2 \pm 0.2$	$1.5 \pm 0.2$
CaT (2) ( $\sigma = 0$ )	$3.4 \pm 0.2$	$1.7 \pm 0.2$	$3.0 \pm 0.4$	$3.8 \pm 0.1$	$3.5 \pm 0.3$	$2.8 \pm 0.1$	$3.8 \pm 0.4$	$2.0 \pm 0.2$	$3.8 \pm 0.3$
CaT (3) ( $\sigma = 0$ )	$3.1 \pm 0.2$	$1.3 \pm 0.2$	$2.7 \pm 0.4$	$3.1 \pm 0.1$	$3.5 \pm 0.4$	$2.8 \pm 0.1$	$3.5 \pm 0.4$	$2.3 \pm 0.2$	$2.5 \pm 0.3$
CaT (2 + 3) ( $\sigma = 0$ )	$6.5 \pm 0.3$	$3.0 \pm 0.4$	$5.7 \pm 0.7$	$6.8 \pm 0.2$	$7.0 \pm 0.6$	$6.1 \pm 0.2$	$7.3 \pm 0.8$	$4.3 \pm 0.4$	$6.2 \pm 0.5$

[S III]  $\lambda 9069$  were measured to determine the velocity dispersion of the gas in the NLR. Three different methods were used.

(i) A suitable continuum was chosen three times by visual inspection and a Gaussian fitted to the whole line. The average of the measurements was obtained and the error calculated as the dispersion of these measurements, thus, the error is associated with the continuum determination. We called the width so obtained  $\sigma_{0h}$ .

(ii) A second value ( $\sigma_{0.2h}$ ) was obtained by fitting a Gaussian, only using the points over  $0.2h$  in the fitting ( $h$  = total height of the line above the continuum).

(iii) The third value ( $\sigma_{0.5h}$ ) was obtained by fitting the core of the line, but this time only using points over  $0.5h$ . The linewidth was calculated with

$$\sigma_v = \sqrt{\sigma^2 - \sigma_i^2}$$

where  $\sigma$  is the dispersion of the Gaussian fitted to each line and  $\sigma_i$  is the instrumental width obtained from measurements of sky emission lines.

The pure emission spectrum was extracted for NGC 4235 and Mk 270 (see Section 4.1.3), and the emission linewidths were measured on them. In the Seyfert 1 and 1.5 of the sample, the widths of the broad ( $\sigma_b$ ) and narrow ( $\sigma_n$ ) components of  $H\beta$  were measured.

#### 4.2.3 Results

The measured emission linewidths are shown in Tables 6 and 7. The widths of the line cores are used in the discussion (i.e.  $\sigma_{0.2h}$ ).

The stellar velocity dispersions (from the Mgb and CaT stellar features) are given in Table 8. Column 4 shows the average value of both measurements ( $\sigma_*$ ). Although  $\sigma_*$  does not have a clear physical meaning, as the Mgb and CaT features can be produced by different stellar populations with different kinematical behaviour, the measurements obtained from the Mgb and from

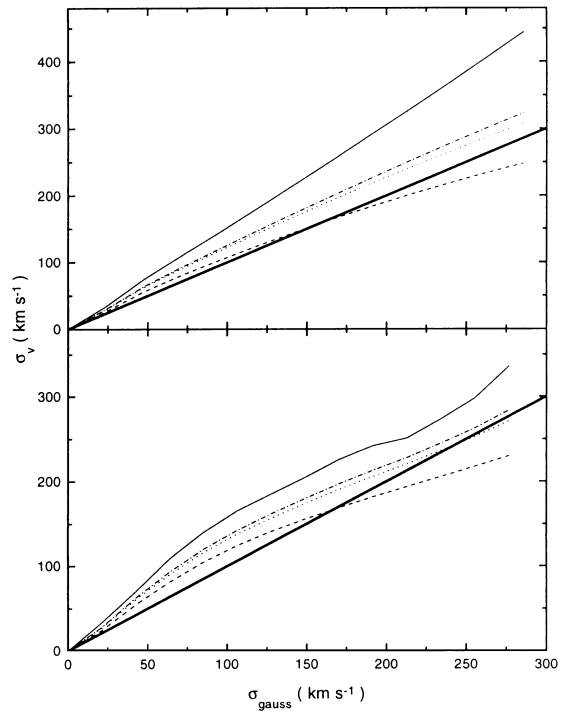


**Figure 5.** Velocity dispersion ( $\sigma_v$ ) of a broadened stellar spectrum, obtained by cross-correlation with a stellar template, versus the widths of the Gaussians used to convolve it ( $\sigma_{\text{gauss}}$ ). The values obtained from filtered functions (dotted and dashed lines) are closer to the real widths (thick straight line) than the values obtained from non-filtered functions (thin line), both for the near-infrared (upper panel) and blue (lower panel) spectra.

the CaT are consistent in all galaxies, except in Mk 1098, 3C 305 and, marginally, in Mk 423. In these three galaxies our measurements point to the presence of, at least, two distinct populations in their nuclei.

**Table 6.** Blue emission linewidths.

Galaxy	[O III] $\lambda 5007$			[O III] $\lambda 4959$			H $\beta$	
	$\sigma_{0h}$ (km s $^{-1}$ )	$\sigma_{0.2h}$ (km s $^{-1}$ )	$\sigma_{0.5h}$ (km s $^{-1}$ )	$\sigma_{0h}$ (km s $^{-1}$ )	$\sigma_{0.2h}$ (km s $^{-1}$ )	$\sigma_{0.5h}$ (km s $^{-1}$ )	$\sigma_n$ (km s $^{-1}$ )	$\sigma_b$ (km s $^{-1}$ )
NGC 4235	196 $\pm$ 3	185 $\pm$ 8	151 $\pm$ 10	226 $\pm$ 25	146 $\pm$ 18	131 $\pm$ 24	–	–
NGC 5940	169 $\pm$ 4	167 $\pm$ 6	151 $\pm$ 8	213 $\pm$ 5	220 $\pm$ 17	169 $\pm$ 19	260 $\pm$ 100	$\sim$ 1960
NGC 6104	64 $\pm$ 4	60 $\pm$ 6	57 $\pm$ 7	61 $\pm$ 6	55 $\pm$ 12	49 $\pm$ 16	91 $\pm$ 29	$\sim$ 3940
Mk 270	178 $\pm$ 2	174 $\pm$ 3	155 $\pm$ 3	188 $\pm$ 6	172 $\pm$ 4	165 $\pm$ 5	185 $\pm$ 3	–
Mk 423	198 $\pm$ 3	204 $\pm$ 8	210 $\pm$ 13	224 $\pm$ 13	200 $\pm$ 21	192 $\pm$ 33	159 $\pm$ 7	–
Mk 759	107 $\pm$ 6	107 $\pm$ 23	103 $\pm$ 31	–	–	–	49 $\pm$ 6	–
Mk 766	142 $\pm$ 8	132 $\pm$ 3	106 $\pm$ 4	126 $\pm$ 5	122 $\pm$ 4	90 $\pm$ 6	121 $\pm$ 13	$\sim$ 785
Mk 885	97 $\pm$ 4	83 $\pm$ 8	66 $\pm$ 10	119 $\pm$ 8	93 $\pm$ 17	68 $\pm$ 22	217 $\pm$ 69	$\sim$ 2565
Mk 1098	121 $\pm$ 5	123 $\pm$ 7	115 $\pm$ 10	128 $\pm$ 8	138 $\pm$ 22	114 $\pm$ 21	164 $\pm$ 49	$\sim$ 1210
3C305	231 $\pm$ 4	224 $\pm$ 8	206 $\pm$ 13	271 $\pm$ 9	242 $\pm$ 22	210 $\pm$ 33	–	–

**Table 7.** Emission linewidths in the near-infrared spectra.

Galaxy	[S III] $\lambda 9069$		
	$\sigma_{0h}$ (km s $^{-1}$ )	$\sigma_{0.2h}$ (km s $^{-1}$ )	$\sigma_{0.5h}$ (km s $^{-1}$ )
NGC 4235	232 $\pm$ 13	–	–
NGC 5940	–	–	–
NGC 6104	71 $\pm$ 6	–	–
Mk 270	202 $\pm$ 11	201 $\pm$ 13	178 $\pm$ 15
Mk 423	238 $\pm$ 24	–	–
Mk 759	36 $\pm$ 9	42 $\pm$ 11	38 $\pm$ 12
Mk 766	114 $\pm$ 3	113 $\pm$ 8	99 $\pm$ 10
Mk 885	125 $\pm$ 18	98 $\pm$ 60	–
Mk 1098	–	–	–
3C 305	201 $\pm$ 33	–	–

**Table 8.** Nuclear stellar velocity dispersions.

Galaxy	$\sigma_*(\text{Mgb})$ (km s $^{-1}$ )	$\sigma_*(\text{CaT})$ (km s $^{-1}$ )	$\langle\sigma_*\rangle$ (km s $^{-1}$ )
NGC 4235	160 $\pm$ 13	153 $\pm$ 8	155 $\pm$ 10
NGC 5940	112 $\pm$ 26	93 $\pm$ 27	103 $\pm$ 27
NGC 6104	144 $\pm$ 23	135 $\pm$ 15	138 $\pm$ 18
Mk 270	137 $\pm$ 11	139 $\pm$ 8	138 $\pm$ 10
Mk 423	167 $\pm$ 17	151 $\pm$ 11	156 $\pm$ 13
Mk 759	65 $\pm$ 10	70 $\pm$ 8	68 $\pm$ 9
Mk 766	106 $\pm$ 40	–	106 $\pm$ 40
Mk 885	145 $\pm$ 16	144 $\pm$ 13	144 $\pm$ 15
Mk 1098	77 $\pm$ 13	122 $\pm$ 15	96 $\pm$ 23
3C 305	212 $\pm$ 24	170 $\pm$ 13	180 $\pm$ 21

## 5 DISCUSSION

### 5.1 Dilution of the nuclear spectral indices

In active galaxies, the EWs of the blue-optical stellar absorption features are smaller than those found in non-active galaxies of the same morphological type. This effect has been called ‘dilution’ in the literature, where it is assumed to be caused by the BFC emitted by the AGN. Nevertheless, a nuclear featureless continuum is not necessary in order to explain why the EWs of the blue indices are small in active galaxies. According to stellar population models, the blue indices of a young and/or low metallicity stellar population are also much smaller than the indices of the high metallicity nuclei of early-type galaxies without active star formation. In this case, of course, the word ‘dilution’ is not suitable as the indices are not diluted by any BFC, they are intrinsically weak.

Nevertheless, we can define the effective dilution of an absorption feature in a galactic spectrum as the ratio between the EW of the feature in that galaxy and the average EW of the index in normal galaxies of the same morphological type:

$$D_{\text{Index}} = \frac{\text{EW}_{\text{Index}}}{\langle \text{EW}_{\text{Index}} \rangle}.$$

This effective dilution is not real, in the sense that it has not been caused by a power-law featureless continuum, but it is useful to quantify the different effects that reduce the EWs of the spectral indices of a galaxy.

In summary, the dilution of the optical stellar features in Seyfert galaxies is explained in different ways.

(i) In the *standard* model, the continuum emitted by the nucleus of a Seyfert galaxy is dominated by the featureless continuum emission from the AGN that dilute the stellar spectral indices from the bulge stars.

(ii) If there are luminous starbursts in the central region of a Seyfert galaxy, the EWs of the blue absorption features, such as the Mgb or the Fe indices, will be weak as in the spectra of hot young stars. Therefore, the observed optical continuum would be fairly featureless as is the case in starburst galaxies (TDT90; Cid Fernandes & Terlevich 1995). In the case of Seyfert 1 galaxies, the broad emission lines of the BLR represent an extra source of dilution that must be taken into account.

(iii) In general, the lower the metallicity of a galaxy and the weaker its stellar features are, the smaller the EWs. It is unlikely that the central regions of early-type galaxies, which commonly host Seyfert nuclei, are of low metallicity so we will not consider this third possibility further.

There are several methods to discriminate between which of these effects causes the dilution in the blue-optical spectrum of a certain galaxy. We have followed TDT90 and compared the nuclear effective dilution of the Mgb index ( $D_{\text{Mgb}}$ ) with the observed effective dilution of the CaT ( $D_{\text{CaT}}$ ). If the light emitted by the AGN is responsible for the dilution,  $D_{\text{blue}}$  and  $D_{\text{CaT}}$  would follow a simple relation, because the emission from the AGN follows a power law:  $F_\lambda \propto \lambda^{-\alpha}$  (with  $0.8 \gtrsim \alpha \gtrsim 1.7$ ). On the other hand, if the blue indices are weak because of the presence of young stars in the nucleus, the CaT could be strong, as the CaT feature is strong in young red supergiants.

To measure the effective dilution of the stellar features in the spectra of Seyfert galaxies, a reference value for the EWs of these features in normal non-active galaxies is needed. Unfortunately, such a reference value is not well established. Galactic spectral

indices depend on the age and metallicity of the stellar populations in that galaxy; therefore, the EWs of the indices in normal galaxies show a wide range of values. To limit that range we must choose template galaxies of the same type as the ones in this study. Strictly speaking, templates should have the same redshift and morphological properties (Hubble type, bulge magnitude, etc.) as the observed galaxies, but this is not always possible. As Seyfert galaxies are preferentially found among early-type spirals (Ho, Filippenko & Sargent 1997), we have searched the literature for samples of these galaxies with measured spectral indices. Reference values for the blue indices were obtained from Idiart, de Freitas Pacheco & Costa (1996) and Fisher, Franx & Illingworth (1996), which were chosen because their samples contained a substantial number of early-type non-active spiral galaxies, and because the methods they used to measure the EWs were the same as our method. We have selected the galaxies with Hubble types between Sb ( $T = 3$ ) and E/S0 ( $T = -3$ ). A total number of 62 galaxies were used. The reference values were calculated taking the median of the EWs of the lines in these galaxies and are shown in Table 9. Using the larger (more than 500 galaxies) – but also far more inhomogeneous – sample of Bica et al. (1991), we obtain a similar average value for Mgb ( $3.9 \text{ \AA}$ ).

To find the average value of the EW of the CaT in normal spirals, we chose the galaxies with  $-3 \leq T \leq 3$  from TDT90, and obtained, taking the median, a reference value of  $7.6 \pm 0.8$ . This value is more uncertain than the one for Mgb, because we only used eight galaxies to calculate it. Theoretical models (García-Vargas, Mollá & Bressan 1998) predict that the CaT of an old ( $t \geq 2 \text{ Gyr}$ ) single stellar population of solar metallicity should have an EW between 7 and 9 Å, depending on the model chosen, which agrees with our reference value.

Although we believe that these average values are reasonably good, there is a large scatter in the EWs of the indices in normal early-type spirals. The EW of the Mgb index can be as low as 2 Å, or as high as 5 Å. Mgb EWs higher than 5 Å are not common in spirals but they are in ellipticals. The range of values covered by the EW(CaT) is not so wide, usually between 6 and 8.5 Å in spirals.

$D_{\text{Mgb}}$  versus  $D_{\text{CaT}}$  are presented in Fig. 6. Five Seyfert 1 galaxies of the present sample and two Seyfert 1s from the TDT90 sample have been included in this figure. Whereas TDT90 measured the CaT for these two galaxies, the Mgb values are from Dahari & De Robertis (1989). We can see the galaxies separating into two different groups: in the first group (group I: NGC 4235, NGC 6104 and Mk 885) the EWs fall into the range of values covered by the indices of normal spiral bulges. These galaxies also share other properties:

- (i) the emission from the BLR is weak, with  $\text{EW}(\text{H}\beta_{\text{broad}}) \geq -40 \text{ \AA}$ ;
- (ii) they are not Fe II emitters;
- (iii) their nuclei are spatially resolved (Malkan et al. 1998).

In summary the Seyfert activity in these galaxies appears to be weak. Our spectra, because of their poor spatial resolution,

include, not only the nuclei of the galaxies, but also, at least partially, their bulges. For these reasons we believe that, in these galaxies, the emission from the old stellar population in the bulge is masking the continuum emission from the active nucleus.

The galaxies of the second group (group II: NGC 3516, NGC 3227, NGC 5940 and Mk 1098) are far more active: they have a prominent BLR with  $\text{EW}(\text{H}\beta_{\text{broad}}) \leq -45 \text{ \AA}$ , they are very strong Fe II emitters and their nuclei are not spatially resolved. The spectral indices of these galaxies, both the blue ones and the CaT, are diluted thereby exhibiting the contribution of an additional continuum over that corresponding to a ‘normal’ galaxy nucleus. However, the relation between the dilutions of the blue indices and the CaT does not conform to the predictions of the standard model, in which the continuum emitted by the AGN follows a power law. In these four galaxies the dilution of the blue indices is relatively greater than the dilution of the CaT. There are two possible explanations for this: the presence of a compact nuclear starburst in the nuclei of these galaxies and/or the dilution of their blue indices by Fe II multiplet emission.

NGC 3516 seems to be the most extreme case: only the blue indices are diluted. The CaT is, instead, slightly enhanced with respect to the values found in normal galaxies. Nevertheless, other observations (Serote-Roos et al. 1996) suggest that the CaT may be somewhat diluted in the nucleus of NGC 3516, at least if we take the EW of the CaT in the bulge of this galaxy as a reference value.

The redshift range covered by our sample (0.007–0.041) implies different total areas for the fixed 10-pixel extraction in each galaxy, between 0.08 and 1.7  $\text{kpc}^2$ . The results presented here are nevertheless barely affected by this as the Seyfert 1 nuclear luminosity dominates the spectra, which is evidenced by the fact that the BLR shows up prominently even in the outermost pixels of the extraction windows. In any case, contamination by bulge stars would tend to decrease the dilution of the Mgb and the CaT in the same proportion.

Circumnuclear star-forming regions cannot be ruled out in many Seyfert 1s as it is not possible to resolve the inner 200–500 pc with ground based telescopes as a result of their large distances from the Earth.

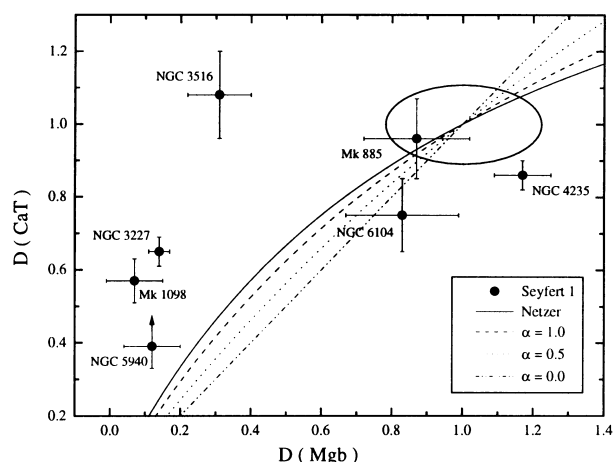


**Figure 6.** Dilution of the CaT versus dilution of the Mgb indices. The lines represent different power laws for the continuum  $F_{\lambda} \propto \lambda^{-\alpha}$ . The solid line represents a model (Netzer 1990) with two values of  $\alpha$ , a value for the blue and another value for the near-infrared. The ellipse shows the range of values covered by early-type galaxies. The galaxies inside or near the ellipse are, therefore, not diluted with respect to normal spirals.

**Table 9.** Reference values for the atomic indices.

Mgb EW(Å)	Fe <sub>52</sub> EW(Å)	Fe <sub>53</sub> EW(Å)	CaT (2 + 3) EW(Å)
$3.8 \pm 0.8$	$2.8 \pm 0.6$	$2.6 \pm 0.6$	$7.6 \pm 0.8$

### 5.1.1 Young starbursts in the nuclei of Seyfert 1 galaxies

All Seyfert 2 galaxies observed until now with good spatial resolution at ultraviolet wavelengths show nuclear starbursts (Heckman et al. 1997; González Delgado et al. 1998). Thus, if unified models were correct, we should also see some starburst signatures in the spectra of Seyfert 1 nuclei. The presence of such starbursts in the nuclei of the group II galaxies could explain our observations, as the CaT is strong in the spectra of young red supergiants. On the other hand, only our luminous Seyfert 1 galaxies have the CaT less diluted, relatively, than the Mgb. If similar starbursts were present in all Seyfert 1 nuclei, we should also see relatively strong CaT features in the nuclear spectra of the weaker Seyferts.

This can be explained by the data on Seyfert 2 galaxies. González Delgado et al. (1998) have found that the bolometric luminosities of the active nuclei and nuclear starbursts in Seyfert 2 galaxies are positively related. If starbursts in Seyfert 1 follow this same relation, the spectral features from young stars in the spectra of the weaker Seyfert 1 could be masked by the old stellar populations of the bulge. On the contrary, in more active Seyferts, the starburst could be strong enough as to increase the EW of the CaT so that it could be seen in spite of the strong continuum emitted by the AGN.

### 5.1.2 Blue indices diluted by Fe II multiplets

One of the common properties of all the galaxies in the group II is that they are strong Fe II emitters. The lines of Fe II [more precisely the bump formed by multiplets (42), (48) and (49)], can mask the Mgb, Fe<sub>52</sub> and Fe<sub>53</sub> stellar features, making these features appear diluted by the continuum emitted by the AGN. If this were true, the dilution of the three blue indices could be very different as the emission of Fe II is very irregular. This could explain why, in some of our galaxies and especially in Mk 1098, the dilution of the Mgb is much greater than the dilution of the Fe indices. On the other hand, the Fe II emission in Seyfert galaxies, seems to be correlated with CaT emission (Persson 1988), i.e. the galaxies that are strong Fe II emitters also show the CaT in emission. This is what happens in Mk 766 and, perhaps, also in Mk 1098. In the other galaxies the CaT could also be in emission at levels too low to be detected but high enough to dilute the EW of the absorption lines.

### 5.1.3 Compact supernova remnants and evolutionary effects

The hypothesis discussed in Sections 5.1.1 and 5.1.2 may actually be compatible with one another, as part of the Fe II emission can be produced by compact supernova remnants (cSNRs) like SN1987F (Filippenko 1989; Wegner & Swanson 1996), SN1988Z (Stathakis & Sadler 1991; Turatto et al. 1993) or SN1997ab (Hagen, Engels & Reimers 1997; Salamanca et al. 1998). These objects are characterized by showing broad permitted emission lines of hydrogen, helium, Fe II and infrared CaT, superposed on a nearly featureless continuum. Their optical spectra are so similar to the spectra of QSOs and type 1 Seyferts that they have been called ‘Seyfert 1 imposters’ by Filippenko. Several explanations have been proposed for the intriguing properties of cSNRs. The most promising are those based on the interaction of the SN ejecta with a dense circumstellar medium ( $n \sim 10^7 \text{ cm}^{-3}$ ; Terlevich et al. 1992a). In the starburst model for AGN of Terlevich et al.

(1992a,b; see also the recent review of Cid Fernandes 1997), the broad permitted emission lines of type 1 Seyfert nuclei are generated by strongly radiative cSNRs in compact nuclear starbursts. In this model, the differences between types 1 and 2 Seyferts are not only a result of obscuration effects but also of the evolution of the central starburst, i.e. an AGN can only become of type 1 when the nuclear starburst has reached a phase at which their most massive stars begin to explode as type II SN (Terlevich, Melnick & Moles 1987). This happens when the burst has an age  $> 8 \text{ Myr}$ .

The starbursts discovered by Heckman et al. (1997) and González Delgado et al. (1998) in four Seyfert 2 galaxies have ages between 3 and 6 Myr. When these massive starbursts reach an age of 8 Myr, they should yield a very high SNe rate. If, as expected from numerical simulations, some of these SN become cSNRs, then these galaxies will, with a high probability, be classified as type 1 AGN.

## 5.2 Gas and stellar kinematics in Seyfert galaxies

Gas in the NLR of Seyfert galaxies can be accelerated by the gravitational field of the galaxy or by violent processes like shock waves or tidal forces. This question has been analysed in several papers (Wilson & Heckman 1985; TDT90; Nelson & Whittle 1996), and all of them have arrived at the following conclusions.

- (i) In the majority of Seyfert galaxies the motion of the gas in the NLR seems to be controlled by the gravitational field of the bulge because the gas and stars show similar velocity dispersions.
- (ii) In some Seyfert 2 galaxies the velocity dispersion of the gas is very high, rising to more than  $400 \text{ km s}^{-1}$ . In these galaxies extra broadening mechanisms must exist. Such mechanisms could be shock waves caused by jets emitted by the active nucleus or gravitational perturbations caused by tidal interactions with other galaxies.

Fig. 7 shows the stellar velocity dispersion versus the width of the emission lines for our new data, together with the values of TDT90. It can be seen in the figure that the majority of the galaxies group around the line with a slope of 1. A least-squares fit gives a correlation coefficient of 0.9 for Seyfert 2 galaxies (after eliminating the points corresponding to NGC 1068 and Mk 78) and only 0.13 for Seyfert 1 galaxies. The slopes of the lines fitted are  $0.48 \pm 0.09$  for Seyfert 2 and  $0.11 \pm 0.32$  for Seyfert 1. Thus, we cannot assert that the stellar and gas velocity dispersions are correlated in Seyfert galaxies.

The galaxies with emission lines much wider than their stellar absorption lines are all Seyfert 2. In these last galaxies, we also observe big differences between the widths of the lines of [O III] and [S III]  $\lambda 9069$ . This points to the existence of several gas clouds in the NLR of these galaxies, each one with different ionization states and moving in different ways. In fact, these clouds have been resolved in NGC 1068 (e.g. Dietrich & Wagner 1998; Kraemer, Ruiz & Crenshaw 1998).

To improve the statistics we added to our data that from Nelson & Whittle (1995). If we plot the width of the [O III]  $\lambda 5007$  emission line versus the stellar velocity dispersion, we would see again a cloud of points around the line of slope 1, but not a clear correlation between both magnitudes. Now, the correlation coefficient is 0.49 for Seyfert 2 and 0.44 for Seyfert 1. The slopes of the lines fitted are  $0.31 \pm 0.09$  and  $0.4 \pm 0.2$  for Seyfert 2 and Seyfert 1 galaxies, respectively. To find out if the clustering

of the data around the slope 1 line really means that the gas motions in Seyfert galaxies are related to the stellar mass of their bulges, we have binned the Seyfert 1 and 2 galaxies separately in stellar velocity dispersion in such a way that there were always more than four galaxies in each group. This results in five groups of type 2 Seyferts and four of type 1. The median of the stellar velocity dispersions of the galaxies in each group versus the corresponding median of their emission linewidths can be seen in Fig. 8. The correlation found between both medians is really surprising. A possible explanation is that the main mechanism that controls the gas motions in the NLR is the gravitational field of the bulge; nevertheless, several other mechanisms might also influence the gas kinematics, therefore the correlation between the gas and stellar velocity dispersion is not evident at first sight. Nelson & Whittle (1996) arrived at this same conclusion by using a more elaborate method of analysis.

Shock waves produced by jets (e.g. Falcke, Wilson & Simpson 1998; Axon et al. 1998) and tidal effects caused by close encounters with other galaxies can disturb and accelerate the gas in the NLR. This could explain why many Seyfert galaxies have emission lines wider than their stellar absorption lines. However, it is more difficult to explain why in many other Seyfert galaxies the emission lines are narrower than the stellar features. The reason could be that, in some galaxies, the gas has settled in a cold rotating disc. This becomes more intriguing if we realize that Seyfert 1 and 2 galaxies show different behaviours in Fig. 8. The medians of the gas velocity in type 2 Seyferts are always higher than the medians of the stellar velocity dispersions, whereas the contrary happens in Seyfert 1s. Fig. 9 represents the ratio between the velocity dispersion of gas and stars in Seyferts, and we can see that, although there is a population of type 2 Seyferts with gas velocities much higher than the velocities of their stars, in Seyfert 1 galaxies there are signs of the existence of another population with inverse kinematical properties. This means that the differences between the kinematical behaviour of Seyfert 1 and 2 galaxies are not likely to be a result of systematic differences between all the galaxies of both groups, but to the existence of these two populations.

There are several possibilities for explaining the different kinematical behaviours of Seyfert 1 and 2 galaxies. If shock waves produced by jets were the main accelerating mechanism of the gas in Seyferts (aside of the gravitational field), the lack of Seyfert 1 galaxies with emission lines much broader than their absorption features could be explained in the context of unified models. According to this model the active nucleus in a Seyfert galaxy is surrounded by a dense molecular torus. Therefore, if the AGN produced radio jets, they would be emitted in a direction perpendicular to the torus plane. The gas in the NLR would also be accelerated in this same direction. Therefore, if the line of sight to the AGN is perpendicular to the torus plane (as, according to unified models, is the case for Seyfert 1 galaxies) we should not see a broadening in the emission lines of the galaxy, but a spectral shift between the stellar and gas emission features.

On the other hand, if the nuclear activity in at least some Seyfert galaxies is produced by gravitational encounters with close companions (e.g. Keel 1996; De Robertis, Yee & Hayhoe 1998), the younger of these Seyferts should also be the ones with broader emission lines. Tidal interactions can disturb and accelerate the gas in the nuclei of the involved galaxies, but, immediately after the encounter, the gas in both galaxies begins to settle again so that in a few Myr the kinematical signs of the interaction will have disappeared. Therefore, the observed differences between the gas

velocity dispersions of Seyfert 1 and 2 galaxies could be explained if nuclear activity were older in Seyfert 1s than in Seyfert 2s.

We could also appeal to morphological differences between Seyfert 1 and 2 galaxies to explain their kinematical behaviour. Seyfert 1s are frequently found in earlier galaxies than Seyfert 2s (Malkan et al. 1998). The gas and stellar velocity dispersions in starbursts found in late-type spirals are of the same order, whereas in early-type starburst galaxies the stellar velocity dispersion

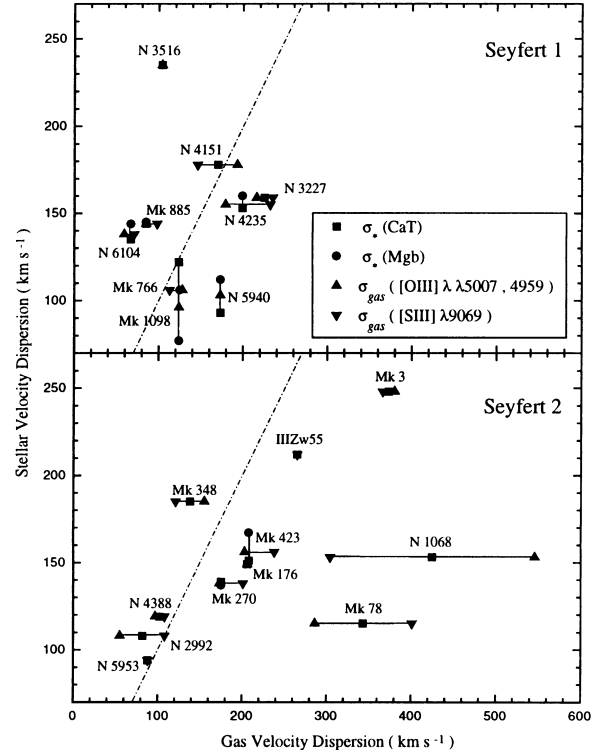


**Figure 7.** Stellar versus gas velocity dispersion in Seyfert galaxies for our new data together with the results from TDT90. There is no clear correlation between the dispersion of the gas in the NLR and that of the stars in the nuclei of Seyferts, although the majority of the galaxies fall around the 1:1 line.

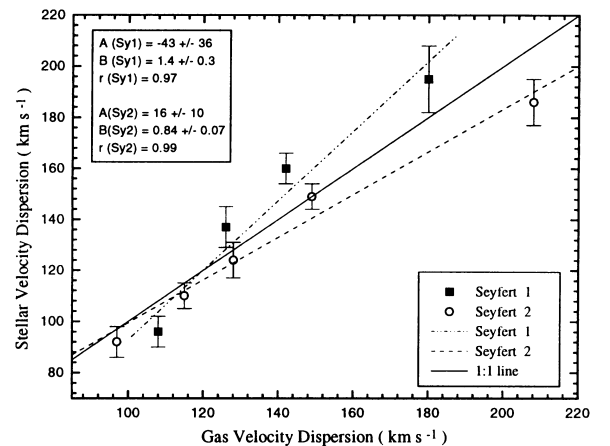


**Figure 8.** Stellar versus gas velocity dispersions for the Seyfert galaxies of TDT90, Nelson & Whittle (1995) and this work. Seyfert 1 and 2 galaxies have been binned in stellar velocity dispersion and the medians of the two magnitudes for each bin are plotted. They are found to be clearly correlated.

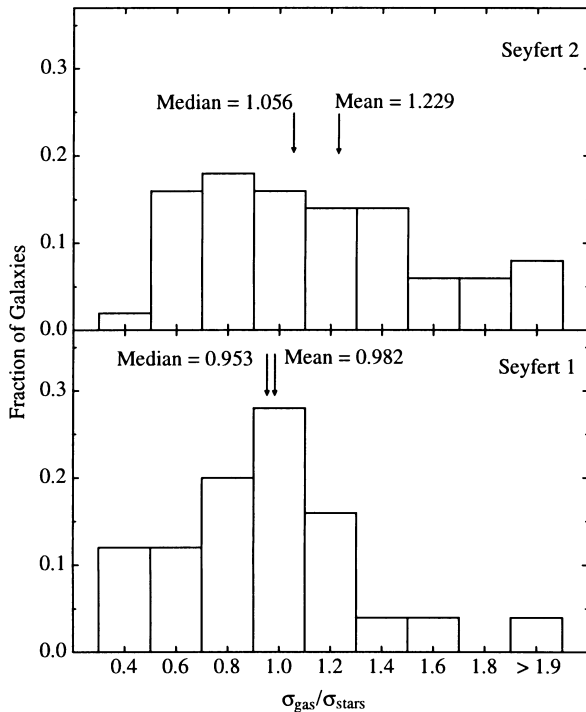


**Figure 9.** Ratio between the gas and stars velocity dispersion in Seyfert galaxies.

seems to be higher than that of the gas (Vega Beltrán et al. 1998). This difference between the gas and stellar kinematics in starburst galaxies could extend to Seyfert galaxies. To test this last possibility, we have compared the differences between the velocity dispersions of the gas and stars in Seyfert galaxies versus their Hubble type and their stellar velocity dispersion (which is a measurement of the bulge mass), but we have not found any clear correlation between these magnitudes. Therefore, we must conclude that it is not likely that the kinematical differences between Seyfert 1 and 2 galaxies are just caused by morphological differences between both types of galaxies.

## 6 CONCLUSIONS

We have studied the CaT and the Mgb stellar absorption indices and kinematics of the nuclei of a sample of 10 active galaxies, focusing our analysis on the study of the properties of Seyfert 1 galaxies.

In spite of problems related to contamination by emission lines, we find that the infrared Ca II triplet stellar indices of Seyfert 1 nuclei, with  $\text{EW}(\text{H}\beta_{\text{broad}}) \lesssim -45 \text{ \AA}$ , are stronger than the values that the standard model would predict from the observed strength of the Mgb index.

This result is naturally explained by the presence, in the nuclei of these type 1 Seyferts, of young stellar clusters the luminosities of which are somehow related to the luminosity of the active nucleus itself. This conclusion is weaker for the nuclei with strong Fe II emission affecting the measurement of the Mgb index.

Our measurements of the velocity dispersions in Seyfert galaxies support previous conclusions by TDT90 and Nelson & Whittle (1996) that the main factor that controls the gas motions in the NLR of Seyfert galaxies is the mass of the bulge. We also find that other factors may also be important, as the correlation

between the gas and stellar velocity dispersions shows a large scatter. Among the factors that may broaden the emission lines in the NLR, induced motions by shocks are the most likely.

Some differences between the kinematics of Seyfert 1 and Seyfert 2 galaxies have been found. Seyfert galaxies with gas velocity dispersions much larger than that of the stars are preferentially found among type 2. Also we found some Seyfert 1 nuclei with emission lines narrower than the stellar absorption features. Although we have outlined some hypotheses, such as orientation and evolutionary effects, a satisfactory explanation for this second aspect still needs to be found.

## ACKNOWLEDGMENTS

We would like to thank Itziar Aretxaga, Javier Gorgas, Enrique Pérez, Javier Palacios and Juan Carlos Vega for many helpful suggestions. We also thank the staff at the William Herschel Telescope and the Isaac Newton Group for their assistance and support. ET acknowledges an IBERDROLA Visiting Professorship to Universidad Autónoma de Madrid. LJB thanks the hospitality of Instituto Nacional de Astrofísica, Óptica y Electrónica and of the Guillermo Haro Programme for Advanced Astrophysics during the finalization of this paper. This research has made use of the NASA Astrophysics Data System (ADS) and of the NASA/IPAC Extragalactic Database (NED).

## REFERENCES

- Abell G. O., Eastmond T. J., Jenner C., 1978, *ApJ*, 221, L1
- Antonucci R. R., 1993, *ARA&A*, 31, 473
- Axon D. J., Marconi A., Capetti A., Maccetto F. D., Schreier E., Robinson A., 1998, *ApJ*, 496, 75
- Bica E., Pastoriza M. G., Maia M., da Silva L. A. L., Dottori H., 1991, *AJ*, 102, 1702
- Brotherton M. S. et al., 1999, *ApJ*, 520, L87
- Cardiel N., Gorgas J., Aragón-Salamanca A., 1998, *MNRAS*, 298, 977
- Cid Fernandes R., 1997, *Rev. Mex. Astron. Astrofis.*, 6, 201
- Cid Fernandes R., Terlevich R., 1992, in Filippenko A. V., ed., *ASP Conf. Ser.*, Vol. 31, Relationships between Active Galactic Nuclei and Starburst Galaxies. Astron. Soc. Pac., San Francisco, p. 241
- Cid Fernandes R., Terlevich R., 1993, in Beckman J., Netzer H., Colina L., eds, *The Nearest Active Galaxies*. *Ap&SS*, 205, 91,
- Cid Fernandes R., Terlevich R., 1995, *MNRAS*, 272, 423
- Colbert E. J. M., Baum S. A., Gallimore J. F., O'Dea C. P., Lehnert M. D., Tsvetanov Z. I., Mulchaey J. S., Caganoff S., 1996a, *ApJS*, 105, 75
- Colbert E. J. M., Baum S. A., Gallimore J. F., O'Dea C. P., Christensen J. A., 1996b, *ApJ*, 467, 551
- Colina L., García-Vargas M. L., Mas-Hesse J. M., Alberdi A., Krabbe A., 1997, *ApJ*, 484, L41
- Dahari D., De Robertis M. M., 1989, *ApJ*, 252, 102
- De Robertis M. M., Yee H. K. C., Hayhoe K., 1998, *ApJ*, 496, 93
- de Vaucouleurs G., de Vaucouleurs A., Corwin H. G. Jr., Buta R. J., Paturel G., Fouqué P., 1991, in EDITORS, eds, *The Third Reference Catalogue of Bright Galaxies*. Springer-Verlag, New York
- Díaz A. I., Terlevich E., Terlevich R., 1989, *MNRAS*, 239, 325
- Dietrich M., Wagner S. J., 1998, *A&A*, 338, 405
- Falcke H., Wilson A. S., Simpson C., 1998, *ApJ*, 502, 199
- Filippenko A. V., 1989, *AJ*, 97, 726
- Fisher D., Franx M., Illingworth G., 1996, *ApJ*, 459, 110
- García-Vargas M. L., Mollá M., Bressan A., 1998, *A&AS*, 130, 513
- González Delgado R. M., Pérez E., 1993, *Ap&SS*, 205, 127
- González Delgado R. M., Pérez E., 1996, *MNRAS*, 278, 737
- González Delgado R. M., Pérez E., Tadhunter C., Vílchez J. M., Rodríguez-Espinosa J. M., 1997, *ApJS*, 108, 155

- González Delgado R. M., Heckman T. M., Leitherer C., Meurer G., Krolik J., Wilson A. S., Kinney A., Koratkar A., 1998, *ApJ*, 505, 174
- Goodrich R. W., 1989, *ApJ*, 342, 224
- Gorgas J., Faber S. M., Burstein D., González J., Courteau S., Prosser C., 1993, *ApJS*, 86, 153
- Goudfrooij P., Emsellem E., 1996, *A&A*, 306, L45
- Hagen H. J., Engels D., Reimers D., 1997, *A&A*, 324, L29
- Haniff C. A., Wilson A. S., Ward M. J., 1988, *ApJ*, 334, 104
- Heckman T. M., González-Delgado R. M., Leitherer C., Meurer G. R., Krolik J., Wilson A. S., Koratkar A., Kinney A., 1997, *ApJ*, 482, 114
- Ho L. C., Filippenko A. V., Sargent W. L. W., 1997, *ApJ*, 487, 568
- Idiart T. P., de Freitas Pacheco J. A., Costa R. D. D., 1996, *AJ*, 112, 2541
- Jones J. E., Alloin D. M., Jones B. J. T., 1984, *ApJ*, 283, 457
- Keel W. C., 1996, *AJ*, 111, 696
- Kraemer S. B., Ruiz J. R., Crenshaw D. M., 1998, *ApJ*, 508, 232
- Kukula M. J., Pedlar A., Baum S. A., O'Dea C. P., 1995, *MNRAS*, 276, 1262
- Maiolino R., Ruiz M., Rieke G. H., Keller L. D., 1995, *ApJ*, 446, 561
- Malkan M. A., Gorjian V., Tam R., 1998, *ApJS*, 117, 25
- Maoz D., Koratkar A., Shields J. C., Ho L. C., Filippenko A. V., Sternberg A., 1998, *AJ*, 116, 55
- Molendi S., Maccacaro T., 1994, *A&A*, 291, 420
- Molendi S., Maccacaro T., Schaeidt S., 1993, *A&A*, 271, 18
- Morris S. L., Ward M. J., 1988, *MNRAS*, 230, 639
- Mulchaey J. S., Wilson A. S., Tsvetanov Z., 1996, *ApJS*, 102, 309
- Nandra K., George I. M., Mushotzky R. F., Turner T. J., Yaqoob T., 1997, *ApJ*, 477, 602
- Nelson C. H., Whittle M., 1995, *ApJS*, 99, 67
- Nelson C. H., Whittle M., 1996, *ApJ*, 465, 96
- Netzer H., 1990, in Courvoisier T. J. L., Mayor M., eds, *Active Galactic Nuclei*. Springer-Verlag, Berlin, p. 57
- Nordgren T. E., Helou G., Chengalur J. N., Terzian Y., Khachikian E. D., 1995, *ApJS*, 99, 461
- Oliva E., Origlia L., Kotilainen J. K., Moorwood A. F. M., 1995, *A&A*, 301, 55
- Osterbrock D. E., 1977, *ApJ*, 215, 733
- Osterbrock D. E., 1981, *ApJ*, 249, 462
- Osterbrock D. E., Dahari O., 1983, *ApJ*, 273, 478
- Osterbrock D. E., Pogge R. W., 1985, *ApJ*, 297, 166
- Palacios J., García-Vargas M. L., Díaz A. I., Terlevich R., Terlevich E., 1997, *A&A*, 323, 749
- Persson S. E., 1988, *ApJ*, 330, 751
- Pogge R. W., 1989, *ApJ*, 345, 730
- Rudy R. J., Cohen R. D., Puetter R. C., 1985, *ApJ*, 288, L29
- Salamanca I., Cid Fernandes R., Tenorio-Tagle G., Telles E., Terlevich R., Muñoz-Tuñón C., 1998, *MNRAS*, 300, L17
- Schmitt H. R., Storchi-Bergmann T., Cid Fernandes R., 1999, *MNRAS*, 303, 173
- Serote-Roos M., Boisson C., Joly M., Ward M. J., 1996, *MNRAS*, 278, 897
- Simien F., de Vaucouleurs G., 1986, *ApJ*, 302, 564
- Stathakis R. A., Sadler E. M., 1991, *MNRAS*, 250, 786
- Terlevich E., Díaz A. I., Terlevich R., 1990, *MNRAS*, 242, 271
- Terlevich R., Melnick J., Moles M., 1987, in Khachikian E., Fricke K., Melnick J., eds, *Observational Evidence for Activity in Galaxies*. Reidel, Dordrecht, p. 499
- Terlevich R., Tenorio-Tagle G., Franco J., Melnick J., 1992a, *MNRAS*, 255, 713
- Terlevich R., Tenorio-Tagle G., Rózycka M., Franco J., Melnick J., 1992b, *MNRAS*, 272, 198
- Tonry J., Davis M., 1979, *AJ*, 84, 1511
- Turatto M., Cappellaro E., Danziger I. J., Benetti S., Gouiffes C., Della Valle M., 1993, *MNRAS*, 262, 128
- Ulvestad J. S., 1986, *ApJ*, 310, 136
- Ulvestad J. S., Wilson A. S., 1984a, *ApJ*, 278, 544
- Ulvestad J. S., Wilson A. S., 1984b, *ApJ*, 285, 439
- Vega Beltrán J. C., Pignatelli E., Zeilinger W., Pizzella A., Corsini E., Bertola F., Beckman J. E., 1998, in Merritt D. R., Valluri M., Sellwood J. A., eds, *ASP Conf. Ser., Vol. 182, Galaxy Dynamics*. Astron. Soc. Pac., San Francisco, p. 219
- Veilleux S., 1991, *ApJ*, 369, 331
- Wegner G., Swanson S. R., 1996, *MNRAS*, 278, 22
- Wilson A. S., Heckman T. M., 1985, in Miller J. S., ed., *Astrophysics of Active Galaxies and Quasi-Stellar Objects*. University Science Books, Mill Valley, CA, p. 39
- Xanthopoulos E., De Robertis M. M., 1991, *AJ*, 102, 1980

This paper has been typeset from a  $\text{\TeX/L\AA\TeX}$  file prepared by the author.